Global Journal of Engineering and Technology [GJET].
ISSN: **2583-3359** (Online)
Frequency: Monthly
Published By GSAR Publishers
Journal Homepage Link- https://gsarpublishers.com/journal-gjet-home/

DEVELOPMENT AND NO LOAD CHARACTERISATION OF A PASSIVE GREENHOUSE SOLAR MANURE DRYER

By

[1] Owoh I. P*, [2]Okonkwo W.I, [3]Okeke I.D and [4]Ojike O.
[1,3]National Centre for Energy Research and Development
[2]World Bank African Centre of Excellence for Power and Energy Development[2,4]
[2,4]Department of Agricultural and Bioresources Engineering University of Nigeria, Nsukka, Nigeria

Article History

Received: 25/02/2025
Accepted: 06/03/2025
Published: 10/03/2025

Vol – 4 Issue – 3

PP: - 01-09

Abstract
This study aimed to assess the performance of a locally fabricated passive solar greenhouse for poultry manure drying. A passive greenhouse solar manure dryer of about 21.31 m3 volume was fabricated with 5 mm thick transparent glass at Nsukka (longitude 7.390 N and latitude 6.860 E) in the southeast of Nigeria. The dryer was tested at no load with all the necessary physical parameters measured. The average values of the heat utilization factor and coefficient of performance of the dryer is 0.49 and 0.53 respectively. The dryer maximum stratification temperature of approximately 7 ^{o}C was observed between the topmost and the lowest trays. The maximum dryer temperature of 37.750 °C was obtained during the period due to cloudy sky. The daily average values of convective heat transfer coefficient and radiative heat transfer coefficient were 1.52 W/m^{2}K, 5.8 W/m2K, and 1.6 W/m^{2}K, 5.8 W/m^{2}K for days one and two, respectively; it ranges from 5.4 W/m^2 K to 6.2 W/m^{2}K and 0.95 W/m^2 K to 2.2 W/m^2 K for radiative and convective heat transfer coefficient, respectively. From the obtained results, the dryer was estimated to be about 39.3% faster than the traditional open-sun drying method.

Keywords: Greenhouse, solar dryer, no-load testing, heat utilization factor, coefficient of performance.

1.0 INTRODUCTION

A solar greenhouse dryer is an energy-efficient system designed to dry various agricultural products using solar energy. Greenhouse dryers are solar dryers that generate heat from trapped solar radiation, based on the principles of the greenhouse effect. The glazing materials in greenhouses are usually made of transparent materials such as glass, polythene, and polycarbonate sheets. The transparent glaze material allows the penetration of solar radiation into the greenhouse and causes the temperature inside the greenhouse to increase as more radiation is being trapped (Morad *et al.*, 2017). Drying of agricultural products in greenhouses has been identified to produce better-quality products when compared with open-sun dried products (Semple *et al.*, 2017; Nayak *et al.*, 2013). Greenhouse technologies are essential in agriculture due to their multiple purposes like plant cultivation, aquaculture, low-temperature thin-layer drying, soil solarization, poultry farming, and water treatments (Singh *et al.*, 2018). Passive greenhouse dryers and other passive drying systems do not require fans or blowers for air movement facilitation. The air movement in a passive system is naturally flowing due to thermosiphon resulting from a density difference from the temperature difference within the greenhouse (Patil *et al.*, 2009). According to Singh and Shrivastava (2017), thermal losses in greenhouse dryers affect their efficiency; this implies that the performance of passive greenhouse dryers can be improved by reducing their thermal losses. Other efforts have been made to improve the efficiency of greenhouse dryers, like using mirrors for reflecting infrared radiations (Sethi and Arora 2009), insulation, and inclination of the north wall (Rathore and Panwar (2010); Sevda and Rathore (2010); Panwar *et al.*, 2013; Prakash and Kumar 2014; Singh and Kumar 2016), introduction of heat storage material in the floor (Janjai *et al.*, 2007, Belloulid *et al.*, 2017, Prakash *et al.*, 2016; Ayyappan *et al.*, 2016), etc. using various floor conditions Prakash and Kumar (2014b). The need to contribute measures towards the improvement of the efficiency of greenhouses has necessitated this work.

The objective of this study was to develop a passive greenhouse solar dryer with improved efficiency. The inside floor of the dryer was made of ceramics to reduce losses, while a matte black painted 30 cm high cement block wall was created to increase radiation absorption and heat storage.

*Corresponding Author: Owoh I. P

The room-size solar manure dryer fabricated with locally available materials had a metallic matte black painted chimney to increase thermosiphon. A no-load testing and characterization of the developed dryer was carried out to determine its coefficients of performance, coefficient of diffusivity, heat utilization factor, and heat transfer coefficients under the no-load condition.

2.0 THEORETICAL ANALYSIS

2.1 Thermal and Energy Balance Analysis

The core of a solar greenhouse dryer is the thermal energy balance. The heat gained from solar radiation must be balanced against the heat losses through convection, conduction, and radiation.

2.1.1 Energy Input

The energy input in a passive solar greenhouse comes primarily from solar radiation. The total solar radiation entering the dryer Q_{in} is calculated using equation 1

$$Q_{in} = I_t \times A \times \tau \quad (1)$$

Where I_t is the total solar irradiance in (W/m^2), A is the surface area of the greenhouse exposed to sunlight and τ is the transmissivity of the glaze material (glass).

2.1.2 Heat Losses.

The heat loss in a greenhouse is by convection, radiation, and conduction.

Convection losses to the environment through air movement are given as Q conv. The convective loss is obtained using equation 2

$$Q_{conv} = H \times A \times (T_{in} - T_{out}) \quad (2)$$

where H is the convective heat transfer coefficient, A is the surface area, T_{in} is the temperature inside the dryer, and T_{out} is the ambient temperature.

Conductive heat Losses through the material of the greenhouse structure are given as Q_{cond} and is obtained using equation 3

$$Q_{cond} = \frac{K \times A \times (T_{in} - T_{out})}{d} \quad (3)$$

where K is the thermal conductivity of the greenhouse material, and d is the thickness of the material.

Radiative heat loss occurs as the dryer emits long-wave radiation. The radiative heat loss Q_{rad} is calculated using the Stefan-Boltzmann law stated in equation 4

$$Q_{rad} = \epsilon \times \sigma \times \mathrm{A} \times \left(T_{in}^4 - T_{out}^4\right) \quad (4)$$

where ϵ is the emissivity of the material, and σ is the Stefan-Boltzmann constant.

2.2 Drying kinetics

The drying process is governed by both external conditions (temperature, relative humidity, airflow) and internal properties of the material being dried (moisture content, diffusion coefficients). The following equations govern drying kinetics.

Moisture content is given as equation 5

$$M(t) = M_0 \times e^{(-kt)} \quad (5)$$

where M(t) is the moisture content at time t, M_0 is the initial moisture content, and k is the drying constant (dependent on temperature, airflow, and material properties).

The rate of moisture evaporation is driven by the difference in moisture content between the product surface and the surrounding air

The evaporation rate is given as equation 6

$$E = h_m \times A \times (P_{v,s} - P_{v,a}) \quad (6)$$

where h_m is the mass transfer coefficient, $P_{v,s}$ is the vapor pressure at the product surface and $P_{v,a}$ is the vapor pressure of the surrounding air.

Thermal efficiency which is the efficiency of converting solar energy into heat used for drying is calculated using equation 7

$$\eta_{thermal} = \frac{m \times h_{fg}}{Q_{in}} \quad (7)$$

Where m is the mass of moisture removed, h_{fg} is the latent heat of vaporization, and Q_{in} is the solar energy input.

Drying Efficiency evaluates how efficiently the system removes moisture. It is calculated from equation 8

$$\eta_{drying} = \frac{M_o - M_f}{Q_{in} \times t} \quad (8)$$

where M_0 and M_f are the initial and final moisture content respectively moisture content, Q_{in} is the energy input, and t is the drying time.

3.0 MATERIAL AND METHODS

3.1 Experimental setup

A room-size glass-glazed passive greenhouse solar manure dryer with a black ceramic floor and a matte black painted 30 cm high cement block wall for increased solar radiation absorption and heat storage was developed for manure drying at the University of Nigeria, Nsukka, longitude 7.39^0 N and latitude 6.86^0 E, south-east of Nigeria. The pictorial view of the developed greenhouse solar manure dryer is shown below

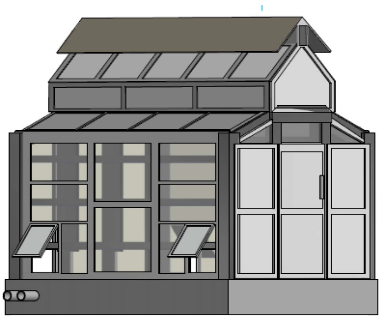

Fig. 3.1. 3D design of the passive greenhouse before construction

Fig. 3.2. Picture of the passive greenhouse after construction

The internal dimensions of the drying system are 3.08 m x 2.09 m x 3.31 m for length, width, and height, respectively.

*Corresponding Author: Owoh I. P

The dryer was formed with a 5 cm and 2.5 cm angle iron for rigidity and firmness. The framework is covered with 5 mm-thick transparent glass that allows direct solar radiation into the drying chamber. Inlet and chimney (outlet) openings measuring 4800 cm2 and 4654 cm2, respectively, were provided for air draft. The dryer consists of a drying chamber made of manure drying trays with a total surface area of 10 m2. The system can handle about 200 kg of poultry manure at a batch using an optimum drying depth of 3 cm for maximum drying efficiency (Ghaly and MacDonald, 2012). A stagnation test was conducted between 8.30 AM and 5 PM on 20 April 2023. Also, no-load testing of the dryer was conducted from 21st June to 23rd June 2023, and all necessary parameters were recorded from 8.30 AM to 5 PM daily

3.2 Instrumentation.

The temperature values at various points were obtained using. Applent AT4208 Multi Channel temperature meter which is capable of measuring up to 8 distinct temperature values concurrently with an accuracy of 0.2%+1°C.

The relative humidity values were obtained using UNI T industrial hygrometer which measures both temperature and relative humidity. Model: UT331.The wind velocity value at the dryer site was obtained using a hot wire anemometer integrated into a personal computer for data logging. The incident solar radiation was measured using Lutron electronic solar power meter model SPM-1116SD with a range of 2000 W/m².

All these instruments were used to study the physical parameters inside and outside the dryer.

3.3 Performance Analysis.

In other to analyze the efficiency of a solar drying system, some important characteristic parameters were evaluated. Such parameters are as follows.

Heat utilisation factor

Heat utilization factor (HUF) which is a ratio of temperature decrease due to cooling of air during drying and temperature increase due to heating of air (Tiwari, 2009) is given as

$$HUF = \frac{(T_{gd}-T_{rm})}{(T_{gd}-T_a)} \qquad (9)$$

Coefficient of performance

Coefficient of performance (COP) is the ratio of the temperature difference between the greenhouse room temperature and ambient temperature to the temperature difference between the ground temperature and ambient temperature (Tiwari, 2009)

$$COP = \frac{(T_{rm}-T_a)}{(T_{gd}-T_a)} \qquad (10)$$

Overall heat transfer coefficient

The overall heat transfer coefficient *(U_O)* can be calculated as follows (Asim Ahmed *et al.*, 2023)

$$\frac{1}{U_o} = \frac{1}{h_1} + \frac{1}{K_{cd}} + \frac{1}{h_{conv}} \qquad (11)$$

$$h_1 = h_{cvt} + h_{eva} + h_{rad} \qquad (12)$$

In no-load experimental conditions, the evaporative losses are negligible thereby making the evaporative heat transfer coefficient to become zero.

h_{eva} = 0. (Singh and Shrivastava, 2017)

Convective heat transfer coefficient

The measure of heat loss through the system to the surroundings is the convective heat transfer coefficient. The convective heat transfer coefficient (HCV) in a passive system is calculated using Prakash and Kumar (2014a), Singh and Kumar (2012a), and Kumar and Tiwari (2006a)

$$h_{cvt} = 0.884 \times \left[(T_{gd} - T_{rm}) + \frac{[P(T_{gd}) - Rh_a P(T_{rm})](T_{rm}+273)}{268900 - P(T_{gd})}\right]^{1/3} \qquad (13)$$

T_{gr} and T_{rm} are the greenhouse ground and room temperature respectively

P(T) is the saturation vapor pressure at temperature T and is given (Huang 2018)

$$P(T) = \frac{\exp(34.494 - \frac{4924.99}{T+237.1})}{(T+105)^{1.57}} \qquad (14)$$

$$h_{conv} = 7.2 + 3.8V_a \qquad (15)$$

Radiative heat transfer coefficient

Substituting accordingly in equation (4)

$$h_{rad} = \frac{\sigma\epsilon\left[(T_{gd}+273.15)^4 - (T_{rm}+273.15)^4\right]}{(T_{gd}-T_{rm})} \qquad (16)$$

Where ϵ is the emissivity of the glass used and is given as 0.89 and σ is Stefan Boltzmann constant.

The characteristic length of the dryer (X) is given as X = $\frac{L+W}{2}$ (17)

The thermal conductivity of air at temperature (Ti) is given as

$$K_{cd} = 0.0244 + 0.6773 \times 10^{-4} Ti \qquad (18)$$

Where Ti is the average temperature of the dryer air and ground temperature

$$Ti = \frac{T_{gd}+T_{rm}}{2} \qquad (19)$$

4.0 RESULTS AND DISCUSSION

3.1 Stagnation test.

A stagnation test was carried out and the temperature and relative humidity values were collected and recorded through data loggers. The summary of the result obtained from the stagnation test (Table 3.1) shows that a maximum stagnation temperature (MST) of 48.94^{0}C was attained by 3.42 pm on 20th April 2023.The results were as follows;

Table 4.1. Table of experimental results for stagnation test

Drier maximum stagnation temperature (MST)	48.94^{0}C
Drier relative humidity at MST	49.7%
Ambient temperature at MST	32.32^{0}C
Ambient relative humidity at MST	31.4%

*Corresponding Author: Owoh I. P

Solar radiation at MST	893.52w/m^2

4.2 No Load test.

The findings of the two days of no load testing were evaluated and reported as follows;

Table 4.2. Summary of experimental results

S/N	Parameters	Day 1	Day 2	Average
1	Maximum dryer temperature	37.07	34.29	35.68
2	Minimum dryer temperature	26.32	26.71	26.51
3	Mean dryer temperature	31.42	31.63	31.52
4	Maximum ambient temperature	33.2	35.75	34.47
5	Minimum ambient temperature	25.52	12.66	19.09
6	Mean ambient temperature	28.55	27.91	28.23
7	Maximum dryer ground temperature	40.12	46.26	43.19
8	Minimum dryer ground temperature	27.26	27.78	27.52
9	Mean dryer ground temperature	34.03	35.75	34.89
10	Mean ambient ground temperature	30.24	27.9	29.07
11	Maximum dryer RH	76.3	72.8	74.55
12	Minimum dryer RH	26.6	25.9	26.25
13	Mean dryer RH	40.5	35.53	38.02
14	Maximum ambient RH	83.4	87.6	85.5
15	Minimum ambient RH	51.5	38.3	44.9
16	Mean ambient RH	66.74	65.01	65.88
17	Maximum stratification	3.76	6.66	5.21
18	Minimum stratification	0.54	1.7	1.12
19	Mean stratification	1.94	2.12	2.03
20	Average heat utilization factor	0.48	0.51	0.49
21	Maximum heat utilization factor	0.88	1.04	0.96
22	Minimum heat utilization factor	0.16	0.10	0.13
23	Average coefficient of performance	0.53	0.48	0.49
24	Average wind speed	0.23	0.42	0.325
25	Mean convective heat transfer coefficient	1.5	1.6	1.55
26	Mean radiative heat transfer coefficient	5.7	5.8	5.75

The dryer was tested at no load with the stratification profile obtained between the topmost and the lowest tray. Figures 3.1a and 3.1b show that the topmost tray has a relatively higher temperature than the middle and the lowest tray. At some points, the temperature of the three trays seems to become equal, this is because of heavy cloud cover which was responsible for the drop in overall dryer temperature. The extent of the temperature difference between the dryer trays for the two days of testing could be observed to be about 2.02^{o}C as the mean stratification temperature. The mean maximum stratification temperature was 5.21^{o}C as seen in Table 3.1 also the maximum stratification temperature of 6.66^{0}C which was obtained on day 2 is within the range of value obtained by (Soumaïla *et al*.,2022) with the drying chamber maximum stratification temperature value of 6.9 °C. The graph of temperature distribution within the dryer trays is shown below (figure 4.1)

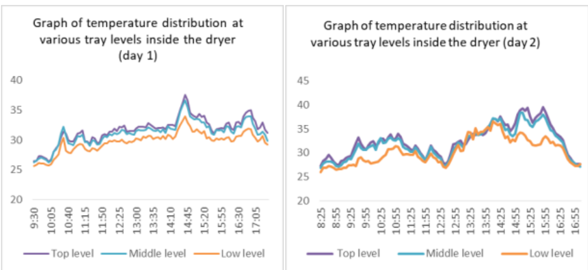

Fig. 4.1. Graph of temperature distribution at the various tray levels inside the dryer

The airflow inside a dryer prohibits stratification, this can be seen from the low stratification in active solar drying systems hence this necessitates the investigation of the relation between stratification and ambient wind speed in a passive greenhouse dryer. Figure 4.2 is the graph of wind speed and stratification. The graph did not show a clear direct relationship between wind speed and stratification but there seems to be an inconsistent inverse relationship between them.

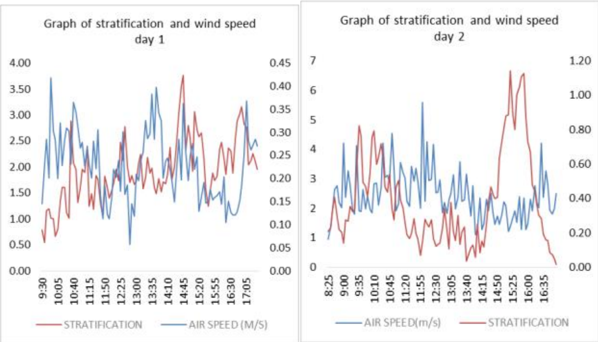

Fig. 4.2. Graph of dryer temperature stratification and wind speed

The graph of stratification and dryer ground temperature shows a similarity in progression thereby suggesting that stratification increases with increase in ground temperature. This could be seen from figure 4.3

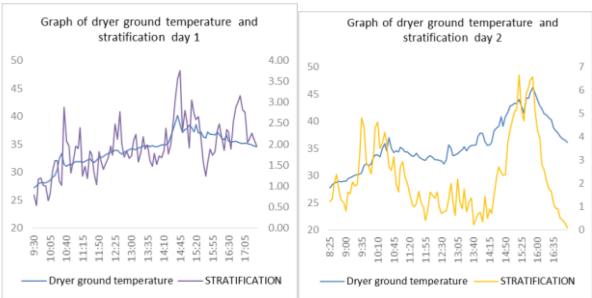

Fig 4.3. Graph of dryer ground temperature and stratification

From figure 4.4, and also table 4.2, the mean ambient temperature was 28.23^{0}C while the mean dryer temperature was 31.52. The difference between the mean dryer temperature and mean ambient temperature for the two days testing period was 3.29^{0}C. The weather was not bright during the testing period but the dryer was observed to attain a maximum dryer temperature of 37.07^{0}C. which is approximately 9^{0}C above mean ambient temperature. The temperature profile between dryer air and ambient is not similar to the result obtained by (Soumaïla *et al*.,2022) whose drying chamber air temperature reached a maximum value of 48.8 °C, which has a difference of 21.5 °C from their outside air temperature. This difference is due to the difference in solar radiation parameters.

The figure 4.4 below has displayed the temperature build up inside the greenhouse. It shows a steady temperature difference between the dryer and ambient. The temperature difference between the dryer and the ambient is a determinant of both the coefficient of performance and heat utilisation factor.

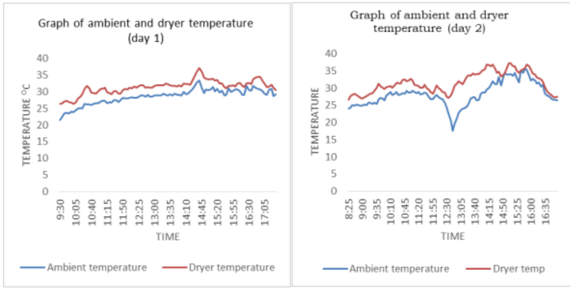

Figure.4.4. Graph of temperature build up inside the dryer with respect to the ambient temperature.

Considering figure 4.4, shows that due to influence of ground temperature the greenhouse room temperature increases (Singh and Kumar, 2016), the black ceramics floor was observed to achieve temperature buildup within the greenhouse. A mean and maximum ground temperature of 34.86^{0}C and 46.26^{0}C respectively was realized with the corresponding mean ambient ground temperature of 29.07^{0}C. This means approximately 20 percent rise in floor temperature at a cloudy weather. When compared with a black painted gravel bed floor (Asim *et al*., 2023) which achieved a maximum room air temperature of 64.4 ◦C, and corresponding heat gain of 53 percent, it means that the black painted gravel may be a better floor considering that the ceramics tiles though black but smooth enough to reflect some radiations back to the atmosphere beyond the greenhouse. The dryer is expected to achieve beyond this on a brighter day

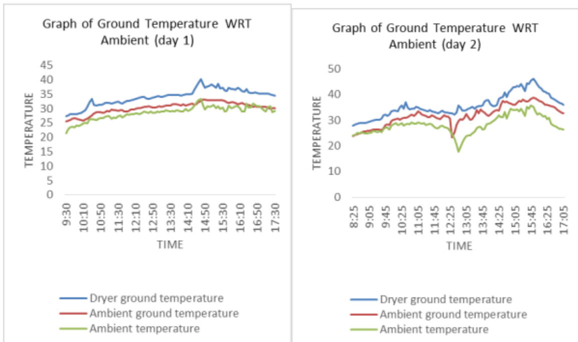

Fig.4. 5. Graph of ground temperatures with respect to ambient temperature

Considering the temperature distribution in figure 3.4 and insolation and temperature relationship in figure 3.6, it shows that both the dryer air temperature and dryer ground temperature are all directly dependent on the value of insolation and this is in agreement with the findings of Singh and Kumar (2016) that ambient temperature, dryer ground and air temperatures increases with global radiation and also decreases with it as well.

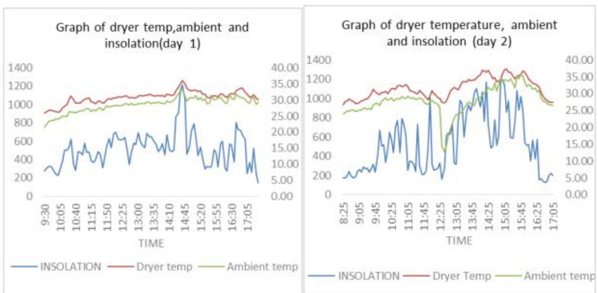

*Corresponding Author: Owoh I. P

Fig 4. 6. Graph showing the relationship between insolation, dryer temperature and ambient temperature.

The graph of coefficient of performance and insolation (figure 4.7) shows that the coefficient of performance also increases as the insolation and vice versa.

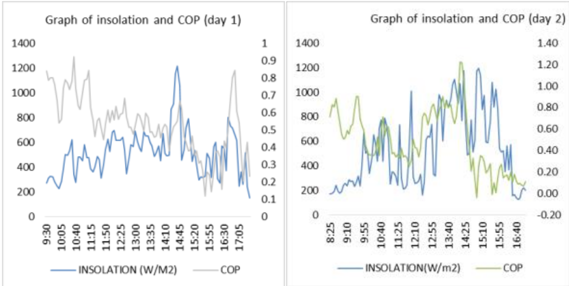

Fig. 4. 7. Graph of the relationship between the insolation and coefficient of performance of the dryer

Figures 4.8a and 48b show that the relative humidity and temperature are inversely proportional to each other both within and outside the dryer. This observation was in agreement with the results of Singh and Kumar (2016) who observed that the increase in dryer temperature brings about the decrease in dryer relative humidity and vice versa.

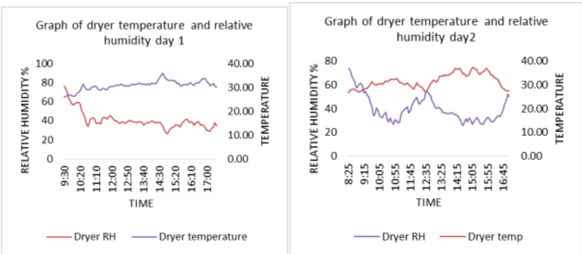

Figure. 4. 8a. Graph of dryer inside temperature and relative humidity

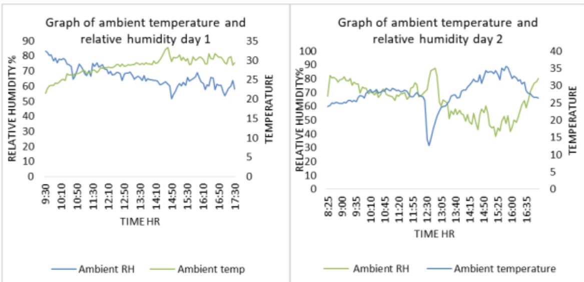

Figure. 4. 8b. Graph of ambient temperatures and relative humidity

The graph of dryer temperature and stratification (figure 4.9) shows that stratification inside a dryer varies as the temperature of the dryer is not directly proportional. It was observed from (figure 4.2) that wind speed also affects stratification in a passive greenhouse. It means that temperature and wind speed are major factors that affect stratification in a greenhouse.

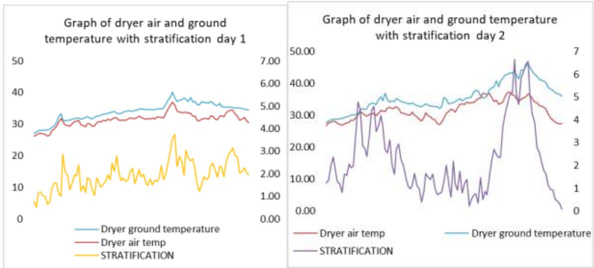

Fig. 4. 8. Graph of stratification between the trays with dryer ground and inside temperature

Figure 4.9 reveals that the value of the dryer heat utilization factor ranges from 0.08 to 0.88 for day 1 and from 0.10 to 0.9 for day 2. The result shows that the obtained values of heat utilization factor are not at variance with the results and values obtained by (Singh and Kumar, 2016) whose values for heat utilization factor varies from 0.107 to 0.616 during experimentation. The observed high heat utilization factor could be a result of the thermal resistive properties of the ceramics material used on the floor.

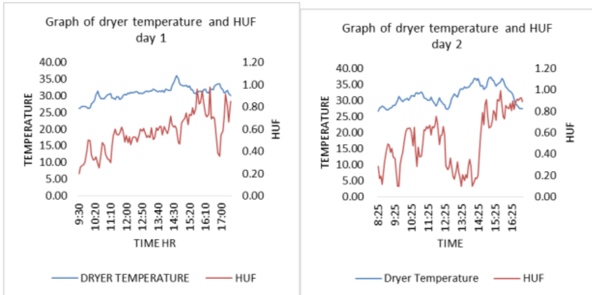

Fig 4. 9. Graph of dryer temperature and heat utilization factor (HUF)

Figure 4.10 shows an alternate trend between the insolation and heat utilization factor. This could be interpreted to represent an inverse relationship between the dryer temperature and the HUF.

Between

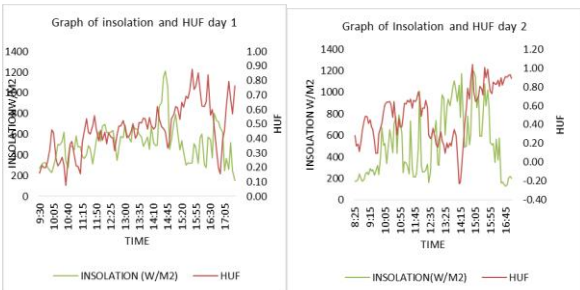

Fig. 4.10. Graph of insolation and heat utilization factor

Considering the convective heat transfer coefficient as shown in figure 4.11, The mean value of the convective heat transfer coefficient for day 1 was 1.5 W/m^2 ^{o}C and ranges from 1.09 W/m^2 ^{o}C to 1.86W/m^2 ^{o}C while the mean value for day 2 was 1.6 W/m^2 ^{o}C and ranges from 0.95W/m^2 ^{o}C to 2.2 W/m^2 ^{o}C When comparing these values with the results obtained by (Ahmed *et al.*, 2023) whose average values for convective heat transfer coefficient was 3.14 m^2 ^{o}C and ranges from 2.47 m^2 ^{o}C to 3.55 m^2 ^{o}C for a passive greenhouse at no load it would be observed that the constructed dryer has shown a

*Corresponding Author: Owoh I. P

good thermal characteristics. Secondly, a comparison between the obtained results and the report of (Jain *et al.,2018*) whose convective heat transfer coefficient was between 2.4 W/m^2 ^{o}C and 2.8 W/m^2 ^{o}C in a direct-type solar dryer. With these comparisons, the constructed passive greenhouse dryer has shown good heat conservation characteristics. The corresponding low values of the convective heat transfer coefficient imply low heat loss from the dryer to the surroundings (Jain *et al.*, 2019)

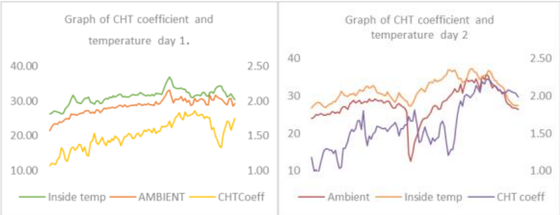

Figure 4.11 Graph of convective heat transfer coefficient and temperature day

Summary of deductions and findings

i. During the testing period, the average relative humidity and temperature inside the greenhouse during the sun hours (six hours for Nsukka longitude 7.390 N and latitude 6.860 E) was found to be 38.02% and 31.52^{0}C while the corresponding values for the ambient relative humidity and temperature were 65.9% and 28.2^{0}C.

ii. From Figure 3.2, the dryer stratification temperature between the trays was found to be decreasing with an increase in ambient wind speed

iii. From Figure 3.8, the dryer stratification temperature between the trays was also found to be proportional to both the dryer ground and average air temperature

iv. From Figure 3.5, the dryer ground and dryer inside temperature varies partly with the value of solar insolation.

v. From Figures 3.9 and 3.10, the insolation was found to have an inverse relationship with the heat utilization factor. It means that the dryer efficiency reduces with an increase in insolation even though the dryer inside air and floor is increasing in temperature

5.0 CONCLUSION AND RECOMMENDATION

This study is focused on the design, fabrication, experimentation, and analysis of a ceramic floor-modified passive greenhouse manure dryer tested in no-load conditions. The primary objective was to localize the fabrication of greenhouse dryers with local materials and with improved floor absorptivity and semi-storage base walls. In carrying out a comprehensive analysis of the experimental data and evaluation of various heat transfer parameters, the following conclusions were drawn: The mean value of convective heat transfer coefficient for day 1 was 1.5 W/m^2 ^{o}C and ranges from 1.07 W/m^2 ^{o}C to 1.86 W/m^2 ^{o}C, while the mean value for day 2 was 1.6 W/m^2 ^{o}C and ranges from 0.89 W/m^2 ^{o}C to 2.3 W/m^2 ^{o}C. When comparing this with the results of Ahmed *et al.*, 2023, whose passive greenhouse tested at no load has a convective heat transfer coefficient that ranges from 2.47 W/m^2 ^{oC} to 3.55 W/m^2 ^{oC} and an average value of 3.14 m^2 ^{oC,} and also when compared with Jain *et al.*, *2018,* who obtained a convective heat transfer coefficient that varies between 2.4 W/m^2 ^{o}C and 2.8 W/m^2 ^{o}C in a direct type solar dryer. The low value of the convective heat transfer coefficient implies low heat loss from the dryer to the surroundings (Jain *et al.*, 2018). The relative low heat loss is due to the high heat utilization factor, which ranges from 0.08 to 0.88 for day 1 and from 0.10 to 0.9 for day 2. The values are not at variance with the range of the findings of Singh and Kumar (2016), whose values for heat utilization factor vary from 0.107 to 0.616 during experimentation. The obtained high maximum heat utilization factor value is due to the insulated and thermally resistive properties of the ceramic floor of the greenhouse.

In conclusion, the locally developed passive greenhouse dryer has proven to be a viable alternative to overcoming the disadvantages of traditional open-sun drying and as a substitute that can contribute to the reduction of the dependence on the use of fossil fuels. The dryer has shown the potential of drying poultry manure considering the temperature and relative humidity profile of the dryer with respect to the ambient conditions. Assuming a quasi-steady state and neglecting the difference in the air velocity between the ambient and inside the dryer, and by adopting the method by Kumar *et al.* *(2013)* with respect to the relative humidity difference, it could be concluded that the dryer could be up to 39.3% faster than the traditional open-sun drying.

Table 4.0 TABLE OF NORMENCLATURE

S/N	SYMBOL	DEFINITION OF SYMBOL
1	HUF	Heat utilisation factor
2	COP	Coefficient of performance
3	U_o	Overall heat transfer coefficient
4	CHT coef	Convective heat transfer coefficient
5	h_{evap}	Evaporative heat transfer coefficient
6	σ	Stefan Boltzman constant.
7	ϵ	Emissivity
8	h_{rad}	Radiative heat transfer coefficient
9	$T_{grd\ inn}$	Greenhouse ground temperature
10	$T_{grd\ out}$	Ambient ground temperature
11	T_{rm}	Greenhouse average room temperature
12	T_{up}	Temperature of the up tray

*Corresponding Author: Owoh I. P

13	T_{middle}	Temperature of the middle tray
14	T_{down}	Temperature of the down tray
15	V_a	Ambient wind velocity
16	L	Length of greenhouse
17	w	Width of greenhouse
18	X	Characteristic length of the greenhouse
19	P(T)	Saturation vapor pressure at temperature (T)
20	Q_{rad}	Radiative heat loss
21	A	The surface Area of the dryer
22	T_{in}	Dryer inside temperature
23	T_{out}	Ambient temperature
24	M(t)	The moisture content at the time (t)
25	k	Drying constant
26	$\eta_{thermal}$	Thermal efficiency

REFERENCES

1. Ahmad, A. et al. (2023) 'Thermal and CFD analyses of sustainable heat storage-based passive greenhouse dryer operating in no-load condition', Sustainability, 15(15), p. 12067. Available at: https://doi.org/10.3390/su151512067.
2. Anil, K. et al. (2013) 'Experimental analysis of greenhouse dryer in no-load conditions', Journal of Environmental Research and development, 7(4).
3. Belloulid, M.O. et al. (2017) 'Solar greenhouse drying of wastewater sludges under arid climate', Waste and biomass valorization, 8(1), pp. 193–202. Available at: https://doi.org/10.1007/s12649-016-9614-1.
4. Ghaly, A.E. and MacDonald, K. N (2012) 'An effective passive solar dryer for thin layer drying of poultry manure', American Journal of engineering and applied sciences, 5(2), pp. 136–150. Available at: https://doi.org/10.3844/ajeassp.2012.136.150.
5. Huang, J. (2018) Simple Accurate Formula for Calculating Saturation Vapor Pressure of Water and Ice College of Chemistry and Chemical Engineering. Wuhan, Hubei, China.
6. Jain, A. et al. (2019) 'Computational fluid dynamics simulation and energy analysis of domestic direct-type multi-shelf solar dryer', Journal of thermal analysis and calorimetry, 136(1), pp. 173–184. Available at: https://doi.org/10.1007/s10973-018-7973-5.
7. Kumar, A. and Tiwari, G.N. (2006) 'Thermal modeling of a natural convection greenhouse drying system for jaggery: An experimental validation', Solar energy (Phoenix, Ariz.), 80(9), pp. 1135–1144. Available at: https://doi.org/10.1016/j.solener.2005.09.011.
8. Morad, M.M. et al. (2017) 'Thermal analysis and performance evaluation of a solar tunnel greenhouse dryer for drying peppermint plants', Renewable energy, 101, pp. 992–1004. Available at: https://doi.org/10.1016/j.renene.2016.09.042.
9. Nayak, S. et al. (2014) 'Energy matrices analysis of hybrid PVT greenhouse dryer by considering various silicon and non-silicon PV modules', International journal of sustainable energy, 33(2), pp. 336–348. Available at: https://doi.org/10.1080/14786451.2012.751914.
10. Panwar, N.L., Kaushik, S.C. and Kothari, S. (2013) 'Thermal modeling and experimental validation of solar tunnel dryer: a clean energy option for drying surgical cotton', International Journal of Low-Carbon Technologies, p. ctt053. Available at: https://doi.org/10.1093/ijlct/ctt053.
11. Patil, R. and Gawande, R. (2016) 'A review on solar tunnel greenhouse drying system', Renewable and Sustainable Energy Reviews, 56, pp. 196–214. Available at: https://doi.org/10.1016/j.rser.2015.11.057.
12. Prakash, O. and Kumar, A. (2014a) 'Environomical analysis and mathematical modeling for tomato flakes drying in a modified greenhouse dryer under active mode', International Journal of food engineering, 10(4), pp. 669–681. Available at: https://doi.org/10.1515/ijfe-2013-0063.
13. Prakash, O. and Kumar, A. (2014b) 'Performance evaluation of greenhouse dryer with opaque north wall', Warme- und Stoffubertragung [Heat and mass transfer], 50(4), pp. 493–500. Available at: https://doi.org/10.1007/s00231-013-1256-2.
14. Rathore, N.S. and Panwar, N.L. (2010) 'Experimental studies on hemi cylindrical walk-in type solar tunnel dryer for grape drying', Applied Energy, 87(8), pp. 2764–2767. Available at: https://doi.org/10.1016/j.apenergy.2010.03.014.
15. Semple, L., Carriveau, R. and Ting, D.S.-K. (2017) 'A techno-economic analysis of seasonal thermal energy storage for greenhouse applications', Energy and buildings, 154, pp. 175–187. Available at: https://doi.org/10.1016/j.enbuild.2017.08.065.
16. Sethi, V.P. and Arora, S. (2009) 'Improvement in greenhouse solar drying using inclined north wall reflection', Solar energy (Phoenix, Ariz.), 83(9), pp. 1472–1484. Available at: https://doi.org/10.1016/j.solener.2009.04.001.
17. Sevda, M.S. and Rathore, N.S. (2010) 'Performance evaluation of the semi-cylindrical solar tunnel dryer for drying handmade paper', Journal of renewable and sustainable energy, 2(1). Available at: https://doi.org/10.1063/1.3302139.
18. Singh, P. and Kumar, A. (2016) 'Performance analysis of greenhouse dryer by using insulated

*Corresponding Author: Owoh I. P

north-wall under natural convection mode', Energy Reports, 2, pp. 107–116.

19. Singh, P. and Shrisvastava, V. (2017) 'Thermal performance assessment of greenhouse solar dryer under passive mode', Journal of Advanced Technology in Engineering and Science, 5, pp. 530–538.
20. Singh, P., Shrivastava, V. and Kumar, A. (2018) 'Recent developments in greenhouse solar drying: A review Renewable and Sustainable Energy Reviews', 82, pp. 3250–3262.
21. Singh, S. and Kumar, S. (2012) 'Development of convective heat transfer correlations for common designs of solar dryer', Energy conversion and management, 64, pp. 403–414. Available at: https://doi.org/10.1016/j.enconman.2012.06.017.
22. Tigampo, S. et al. (2022) 'Experimental characterization of a solar dryer and modelling of the drying kinetics of millet pellets', International Journal of Engineering and Technical Research (IJETR), (12), pp. 2454–4698
23. Tiwari, G.N. (2009) Fundamental of Solar Dryers. New Delhi, India: Anamaya Publishers, pp. 263–264.

*Corresponding Author: Owoh I. P